Submitted for publication

LBL-6743 c.1
Preprint

OBSERVATION OF INTERFERENCE BETWEEN $I_u = 1/2$ AND $I_u = 3/2$ BARYON EXCHANGE AMPLITUDES IN 4 GeV/c BACKWARD INELASTIC SCATTERING

G. Gidal, J. W. Chapman, R. P. Ely,
W. Michael, P. Oddone, and D. Scharre

December 1977

Prepared for the U. S. Department of Energy
under Contract W-7405-ENG-48

LBL-6743

Observation of Interference Between $I_u = 1/2$ and $I_u = 3/2$ Baryon Exchange Amplitudes in 4 GeV/c Backward Inelastic Scattering

G. Gidal, J.W. Chapman†, R.P. Ely, W. Michael, P. Oddone, and D. Scharre‡

Lawrence Berkeley Laboratory
University of California
Berkeley, California

December 1977

ABSTRACT

Interference between the $I_u = 1/2$ and $I_u = 3/2$ baryon exchange amplitudes is observed in the reaction $\pi^- p \rightarrow p\pi^-\pi^o$, with the proton produced forward with $\cos\theta_p^* > 0.8$. The Dalitz plot shows that the reaction is dominated by the quasi two body final states $\rho^- p$(Δ exchange) and $N^{*o}(1670)\ \pi^o$ (N exchange), with $\Delta(1238)$, $N^*(1520)$ and higher mass N^*'s also produced. The relative phase between the ρ and the $N^*(1670)$ production amplitudes is measured to be 135° ±10° and is compared with the Regge pole signature factor phase-predictions.

*This work was done with support from the U. S. Energy Research and Development Administration.

†University of Michigan, Department of Physics

‡Stanford Linear Accelerator Center, Physics Division

The phenomenon of interference between amplitudes leading to the same three body final state has long been known for forward inelastic reactions.[1] Such an interference is usually seen as an enhancement where two resonance bands intersect on the Dalitz plot. These interferences have been most useful in the s-channel analysis of three body final states.[2] To date, they have not provided much information concerning production amplitudes at higher energies.

In this experiment we observe such an interference for the first time in backward inelastic scattering in the reaction

$$\pi^- p \to p\pi^-\pi^0 \qquad (1)$$

and compare the extracted relative phases with the predictions from the Regge pole amplitude signature factor.

A Streamer Chamber spectrometer at the Bevatron was triggered by fast forward protons resulting from 4 GeV/c $\pi^- p$ interactions. A 30 cm liquid hydrogen target was situated within a streamer chamber of dimensions 120 cm x 60 cm x 40 cm in a 13 kg magnetic field. The trigger is provided by two sets of downstream counter hodoscopes which crudely determine the momentum of the forward track. A hard wired coincidence matrix is part of the trigger logic and only allows triggers on positively charged particles with momentum greater than about 1.5 GeV/c. To suppress π triggers, a large aperture, high pressure gas Cherenkov counter placed between the hodoscopes is put in anti-coincidence with the trigger. Beam spark chambers and downstream spark chambers before the first hodoscope are used to improve the resolution on the fast tracks ($\Delta p/p < 1\%$, $\Delta\phi = \Delta\lambda \simeq .04$ deg). A more detailed description of the apparatus is given elsewhere.[3]

Approximately 310,000 measurable frames were exposed, representing a sensitivity of nearly 300 events/μb. The measurements were processed through a modified version of TGVP-APACHE which combines spark chamber and streamer chamber information, finds the production vertex in the target and constrains the events to the appropriate hypotheses. In this paper we report on 90% of this data sample taken from approximately 40,000 2-prong interactions within the target. We select a sample of events which satisfy the 1-C fit to reaction (1) with a confidence level greater than 0.05, which have a proton acceptance greater than 0.15, and for which the missing mass squared is less than 0.25 GeV^2. In Fig. 1a, we show the unweighted Dalitz plot of reaction (1) for 3155 such events with $\cos\theta_p^* > 0.8$, where θ_p^* is the center-of-mass angle of the fast proton with respect to the incident π^-. The proton acceptance decreases with increasing $M_{\pi^-\pi^0}$. We see that the reaction is dominated by the crossing ρ and N^{*0} bands. A fit of the weighted $\pi^-\pi^0$ mass projection (Fig. 1b) with a relativistic Breit Wigner and a polynomial background gives the parameters; $m_\rho = 0.727 \pm 0.007$ GeV and $\Gamma_\rho = 0.168 \pm 0.032$ GeV. This rather low mass and the asymmetric shape of the ρ indicate that an interference phenomenon might be present.

In Fig. 2 we show the acceptance corrected differential cross sections measured[4] in this experiment for the reactions $\pi^-p \rightarrow p\rho^-$ and $\pi^-p \rightarrow N^{*0}(1670)\pi^0$. They are backward peaked demonstrating that these reactions have a dominant baryon exchange production amplitude. In Figure 3a we show the weighted projection of the π^-p mass for $\cos\theta^*_{\pi^-p} > 0.8$, with and without the crossing ρ^- band. We note that the dominant peak appears at a mass of 1670 ± 5 MeV and can be identified with any or all of the several resonances in that mass region.[5] We refer to it as $N^*(1670)$ in this paper. There are also smaller signals that can be identified with the $\Delta(1238)$, $N^*(1520)$ and $N^*(2190)$.

In Fig. 3b we show the $\pi^0 p$ mass projection for $\cos\theta^*_{\pi^0 p} > 0.8$, with and without the dominant ρ^- and $N^*(1670)$ reflections. The $p\rho^-$ and $N^{*+}\pi^0$ final states are manifestly $I_u = 3/2$ exchange, but the N^{*0}'s can be produced by either $I_u = 1/2$ or $I_u = 3/2$ exchange. While the $\Delta(1238)$ and the $N^*(1520)$ appear on both the $\pi^- p$ and $\pi^0 p$ projections, the $N^*(1670)$ and $N^*(2190)$ appear only on the $\pi^- p$ projection. This indicates that the $N^*(1670)$ and $N^*(2190)$ are produced primarily by $I_u = 1/2$ exchange. From a fit to Figs. 3a and 3b, the ratio of the $N^*(1520)$ in the $\pi^0 p$ state compared to the $\pi^- p$ state is (corrected with a Monte Carlo program for relative acceptances) 0.88 ± 0.45. This is to be compared with the ratio 9:4 expected from production by $I_u = 1/2$ exchange, and indicates that the $N^*(1520)$ may be produced by both $I_u = 1/2$ and $I_u = 3/2$ exchange.[6] For the $N^*(1670)$ this same ratio is 0.02 ± 0.04. This translates into an upper limit of 0.012 ± 0.023 for the ratio of $N^{*0}(1670)$ events produced by $I_u = 3/2$ exchange to those produced by $I_u = 1/2$ exchange.[7]

The observation of interference can be made most readily by examining the $\pi^-\pi^0$ mass spectra for several bands of crossing $\pi^- p$ mass and vice versa. These are shown in Figs. 4a through 4h. We notice the rather striking change in shape and amplitude of the ρ^- signal as we pass through the N^* bands. The superimposed curves are the result of the fit described below. We see that they reproduce several characteristic features of the data including the asymmetric ρ peaks, the dip near $M_{p\pi^-} = 2.0$ GeV, and the striking difference in ρ shape and yield below and above $M_{p\pi^-} = 1.650$.

To fit the interference between the resonances, we divide the area of the Dalitz plot (Fig. 1a) within the designated boundaries ($1.6 < M^2_{p\pi^-} \leq 6.0$; $0.2 < M^2_{\pi^-\pi^0} < 1.2$ GeV^2) into a 6×23 element grid. We limit the area over which we fit (and of the projections in Fig. 4) for several reasons: (1) the proton acceptance falls off with increasing $M_{\pi^-\pi^0}$; (2) ambiguities between reaction (1) and other hypotheses, although small, increase with increasing $M_{\pi^-\pi^o}$, (3) overlapping bands of other resonances in the $p\pi^o$ and $p\pi^-$ systems would require additional parameters and complicate the fit. In particular the $\Delta(1238)^{+,o}$ and the $N^*(1520)^+$ are not included in this analysis. Each event is weighted by the proton trigger acceptance and by a geometric correction for steep π^- loss. The number of weighted events in each bin of the grid is fit with the integral of the density of events, N(x,y), over that bin, where (defining $x = M^2_{\pi^-\pi^o}$ and $y = M^2_{\pi^- p}$)

$$N(x,y)\,dx\,dy = |A_\rho + \sum_i A_{N_i^*}|^2 = f_\rho |B_\rho|^2 + \sum_i f_{N_i^*} |B_{N_i^*}|^2$$

$$+ \; 2 \sum_i \xi_i \sqrt{f_\rho f_{N_i^*}}\; |B_\rho||B_{N_i^*}| \cos(\Phi_{N_i^*} - \phi_i - \Phi_\rho)$$

$$+ \; 2 \sum_{i,j} \zeta_{ij} \sqrt{f_{N_i^*} f_{N_j^*}}\; |B_{N_i^*}||B_{N_j^*}| \cos(\Phi_{N_i^*} - \phi_i + \phi_j - \Phi_{N_j^*}) \tag{2}$$

where

$$B_\rho = \frac{\Gamma_\rho m_\rho \sqrt{x^{1/2}/k}}{(x - m_\rho^2) + i\Gamma_\rho m_\rho}, \qquad \tan\Phi_\rho = \frac{-\Gamma_\rho m_\rho}{x - m_\rho^2}$$

$$B_{N_i^*} = \frac{\Gamma_{N_i^*} m_{N_i^*} \sqrt{y^{1/2}/k}}{(y - m_{N_i^*}^2) + i\,\Gamma_{N_i^*} m_{N_i^*}}, \qquad \tan\Phi_{N_i^*} = -\frac{\Gamma_{N_i^*} m_{N_i^*}}{y - m_{N_i^*}^2}$$

The angle $\phi_i \equiv \phi_\rho^{Prod} - \phi_{N_i^*}^{Prod}$ is the difference between the production phases of the ρ and N_i^*, and k is the momentum of the decay π^- in the resonance center of mass. The parameters ξ and ζ can be considered as effective coherence factors, incorporating the overlap of the several helicity amplitudes involved. This expression contains the implicit assumption that all amplitudes leading to the same quasi two-body final state have the same value of ϕ_i.

The s-channel helicity frame decay angular distribution of the N_i^* and the ρ^- are reflected as variations along that resonance band on the Dalitz plot are included as modifications to the Breit-Wigner amplitudes[8] $|B|^2 \rightarrow |B|^2 \, dN/dx$, where $dN/dx = (dN/d\cos\theta^*) \, d\cos\theta^*/dx$. We take $dN/d\cos\theta^* = 1 + a_{15}\cos^2\theta^*$ for the J=3/2 N*(1520); $dN/d\cos\theta^* = 1 + a_{N1} \cos^2\theta + a_{N2}\cos^4\theta^*$ for the presumed J=5/2 N*(1670); $dN/d\cos\theta^* = 1 + a_\rho\cos^2\theta^*$ for the J=1 ρ(760) and $dN/d\cos\theta^* = 1 + a_{21}\cos^4\theta^*$ as an average representation for the higher spin N*(2190).

A minimum chi squared fit of the data to (2) using MINUIT[9] gives the parameters listed in Table I. The results for several sets of assumptions concerning the N_i^* and ρ^- decay angular distributions, and for no interference, are shown. We see that the values of many parameters are rather insensitive to these various assumptions. The procedure is to first fit the resonance masses and widths assuming isotropic angular distributions. The fitted masses and widths of the ρ, N*(1520) and N*(1670) are generally consistent with established values and so the Particle Data Group[5] (PDG) values are used in the fits. The exception is the highest mass N* where the best fit values m=2125 MeV and Γ=160 MeV were used instead. It is clear from the fits that the N^* spectrum above 1700 MeV is not adequately described. There are several resonances in this mass region in the PDG tables. They are all presumably produced and can interfere with the ρ and each other, but the data does not permit including any more parameters. The angular distributions are then included. The data permit a rather wide range of a_i so these are kept fixed in the final fits and error determinations (MIGRAD). The tabulated fits are chosen to illustrate the typical range of variation of the a_i. The $N_i^* N_j^*$ interference term is rather small and was omitted from the fits presented here. The χ^2 for no interference terms at all is always considerably poorer.

We especially discuss the values of the ϕ_i is obtained. In the simple Regge pole theory, the phase of the amplitude is determined by the signature factor $1 + \tau e^{-i\pi(\alpha-1/2)}$ and by the sign of the residue, β.

The baryon exchange Regge phase prediction has previously been roughly verified from the relation between the elastic and charge exchange cross sections at 180 degrees.[10] Amplitude analyses of backward elastic and charge exchange data generally confirm these phases although fits with the simplest model are poor. Most of these fits are characterised by opposite signs of the N and Δ exchange residues, $\beta_N/\beta_\Delta < 0$.[12] For the nominal leading trajectories; $\alpha_{\Delta_\delta} = 0.15 + 0.9u$ $(\tau=-1)$, $\alpha_{N_\alpha} = -0.35 + u$, $(\tau=+1)$ and the average values of u measured for events in each of the N^* bands where they intersect the ρ band, we obtain the production phase difference predictions listed in Table II. Qualitatively, the $N^*(1670)$ amplitude is predicted to lead by 110° (lag by 70°) the ρ production amplitude for positive (negative) relative signs of the residues. This is not quantitatively confirmed by the data, which indicate that the ρ leads the $N^*(1670)$ by about 135° seemingly independent of the various assumptions used in fitting. If we assume that the $N^*(1520)$ is also, as at higher energies,[6] predominantly produced by I=1/2 exchange, then the signs of all the measured phases indicate that $\beta_N/\beta_\Delta < 0$, as in elastic scattering. Absorptive corrections will separately affect each helicity amplitude and presumably complicate this interpretation.

We wish to acknowledge the tireless efforts of our scanning and measuring staff, J. Brannigan and P. Hanson for their help during the running of the experiment, and Drs. H. Haber and P. Hoyer for helpful discussions.

References

1. R. W. Bland, et al. Phys. Rev. Lett. 17, 939 (1966).
A. Fridman, et al. Phys. Lett 21, 462 (1966).
B. Jongejans, Methods in Subnuclear Physics IV, p. 349 (Gordon-Breach, pub. 1970).
W. Michael, Phys. Rev. D7, 1985 (1973).
J. MacNaughton, et al. UCRL-29833 (unpublished).

2. See for example Dalitz and Miller, Phys. Rev. Lett. 6, 562 (1961).

3. D. Scharre, et al. LBL-6150, October 1977 (submitted to Phys. Rev.)
D. Scharre, LBL-6149 (Ph.D. Thesis, April 1977)

4. The background subtracted N^{*o} differential cross section was determined for the entire enhancement $1.45 < M_{p\pi^-} < 1.85$ GeV. The Breit Wigner tail corrections are based on the $N^{*o}(1520)$ and $N^{*o}(1670)$ contributions obtained in a fit to the $p\pi^-$ invariant mass spectrum. We assume I=1/2 and only $N\pi$ decay modes since the identity of these resonances has not been established.

5. Review of Particle Properties, Rev. Mod. Phys. 48, No. 2, Part II, April 1976.

6. A recent experiment at 9 GeV/c sees no evidence of $N^*(1520)$ production by I_u=3/2 exchange; A. Rougé, et al., Phys. Lett. 69B, 115 (1977). We cannot rule out the possibility that the observed $N^{*+}(1520)$ is not produced by baryon exchange.

7. At the two 2σ level this limits the I_u=3/2 production amplitude for the $N^*(1670)$ to less than 12% of the I_u=1/2 production amplitude.

8. Since the proton acceptance limits the N^* decay angles observed to the hemisphere in which the interference occurs, it is difficult to obtain an independent measurement of these a_i. They are not well determined by the fit. This is further complicated by the fact that the events were selected according to $\cos\theta_p^*$ and not $\cos\theta_{\pi^- p}^*$. The $N^*(1670)$ decay distribution in the u-channel helicity frame are generally consistent with the assumed exchanges. The almost isotropic fitted s-channel decay distribution of the ρ^- disagrees with a previous analysis of the same data which ignored interference effects. (Ref. 3 above).

9. F. James and M. Roos, Computer Physics Comm. 10, 343 (1975).

10. V. Barger and M. Olsson, Phys. Rev. D5, 2736 (1972).

11. See for example J. K. Storrow and G. A. Winbow, Nuclear Physics B53, 62 (1973).

12. J. P. Boright, et al. Phys. Rev. Lett. 24, 964 (1970); V. Barger and D. Cline, Phys. Rev. Lett. 19,1504 (1967).

Figure Captions

Fig. 1: (a) Dalitz plot of events fitting reaction (1) with $\cos\theta^*_p > 0.8$; the arrows indicate the boundaries of the region fit.

(b) The $M_{\pi^-\pi^o}$ projection of these events.

Fig. 2: Differential cross sections, $d\sigma/du$, for the reactions $\pi^- p \to p\rho^-$ and $\pi^- p \to N^{*o}$ $(1670)\pi^o$.

Fig. 3: (a) The $M_{\pi^- p}$ spectrum for events with $\cos\theta^*_{\pi^- p} > 0.8$, and (shaded) with the $\rho(760)$ band removed; (b) the $M_{\pi^o p}$ spectrum for events with $\cos\theta^*_{\pi^o p} > 0.8$, and (shaded), with the $\rho(760)$ and N^{*o} (1670) bands removed.

Fig. 4: The $M_{\pi^-\pi^o}$ mass spectra for the successive $M_{p\pi^-}$ mass regions (a) 1.30 - 1.65 GeV, (b) 1.65 - 1.85 GeV, (c) 1.85 - 2.15 GeV, and (d) 2.15 - 2.40 GeV. The $M_{p\pi^-}$ mass spectra for the successive $M_{\pi^-\pi^o}$ mass regions (e) 0.447-0.60 GeV, (f) 0.60 - 0.73 GeV, (g) 0.73 - 0.86 GeV and (h) 0.86 - 1.095 GeV. The curves use the parameters of a type (B) fit (Table I).

TABLE I

	(A)	(B)	(C)	(D)
Assumptions of Fit	$1.3 < M_{p\pi^-} < 2.4$ Isotropic Decays ($a_i = 0$) $\cos\theta_p^* > 0.8$	$1.3 < M_{p\pi^-} < 2.4$ $a_\rho = -0.02$ $a_{15} = -1.1$ $a_{N_1} = 0.88$ $a_{N_2} = 0.74$ $a_{21} = 1.0$ $\cos\theta_p^* > 0.8$	$1.3 < M_{p\pi^-} < 1.85$ $a_\rho = 0.02$ $a_{15} = -1.2$ $a_{N_1} = 1.0$ $a_{N_2} = 0.43$ $\cos\theta_p^* > 0.8$	$1.3 < M_{p\pi^-} < 1.85$ $a_\rho = -0.11$ $a_{15} = -1.0$ $a_{N_1} = 0.80$ $a_{N_2} = 0.80$ $\cos\theta_p^* > 0.9$
χ^2/bins	155/130	136/130	35/52	37/52
$\rho(0.765)$ f_ρ	33.8 ± 2.7	34.6 ± 2.3	45.2 ± 5.7	41.0 ± 5.5
m = 1.520, Γ = 0.120: ξ f φ	0.84 ± 0.78 2.1 ± 1.2 11° ± 19°	0.81 ± 0.24 7.1 ± 2.1 26° ± 23°	0.81 ± 0.19 8.7 ± 2.8 54° ± 22°	0.99 ± 0.75 3.3 ± 1.6 45° ± 20°
m = 1.670, Γ = 0.130: ξ f φ	0.76 ± 0.10 33.6 ± 1.9 126.6° ± 5.7°	0.65 ± 0.10 21.2 ± 1.1 132° ± 6°	0.62± 0.08 20.2± 1.3 138.7°±9.7°	0.66 ± 0.08 16.9 ± 1.1 137.5°±8.0°
m = 2.125, Γ = 0.160: ξ f φ	0.66 ± 0.10 4.6 ± 0.7 141.5°± 9.2°	0.63 ± 0.10 3.8 ± 0.6 143.2°±11.5°		
χ^2 for no interference with same assumptions	240	202	74	72

TABLE II.

	$\langle u \rangle$ GeV^2	I_u	φ^{PROD}_{REGGE}	Predicted φ $(= \varphi^{PROD}_{\rho} - \varphi^{PROD}_{N^*})$	Average Measured φ
$\rho(765)$	-0.160	3/2	-45°, $+135^\circ$	--	--
$N^*(1520)$	0.025	1/2	74.3°	-119.3°, 60.7°	$40 \pm 23^\circ$
		3/2	-60.6°	15.6°, -164.4°	
$N^*(1670)$	0.097	1/2	67.7°	-112.7°, 67.3°	$35 \pm 10^\circ$
$N^*(2125)$	0.191	1/2	59.3°	-104.3°, 75.7°	$143 \pm 12^\circ$

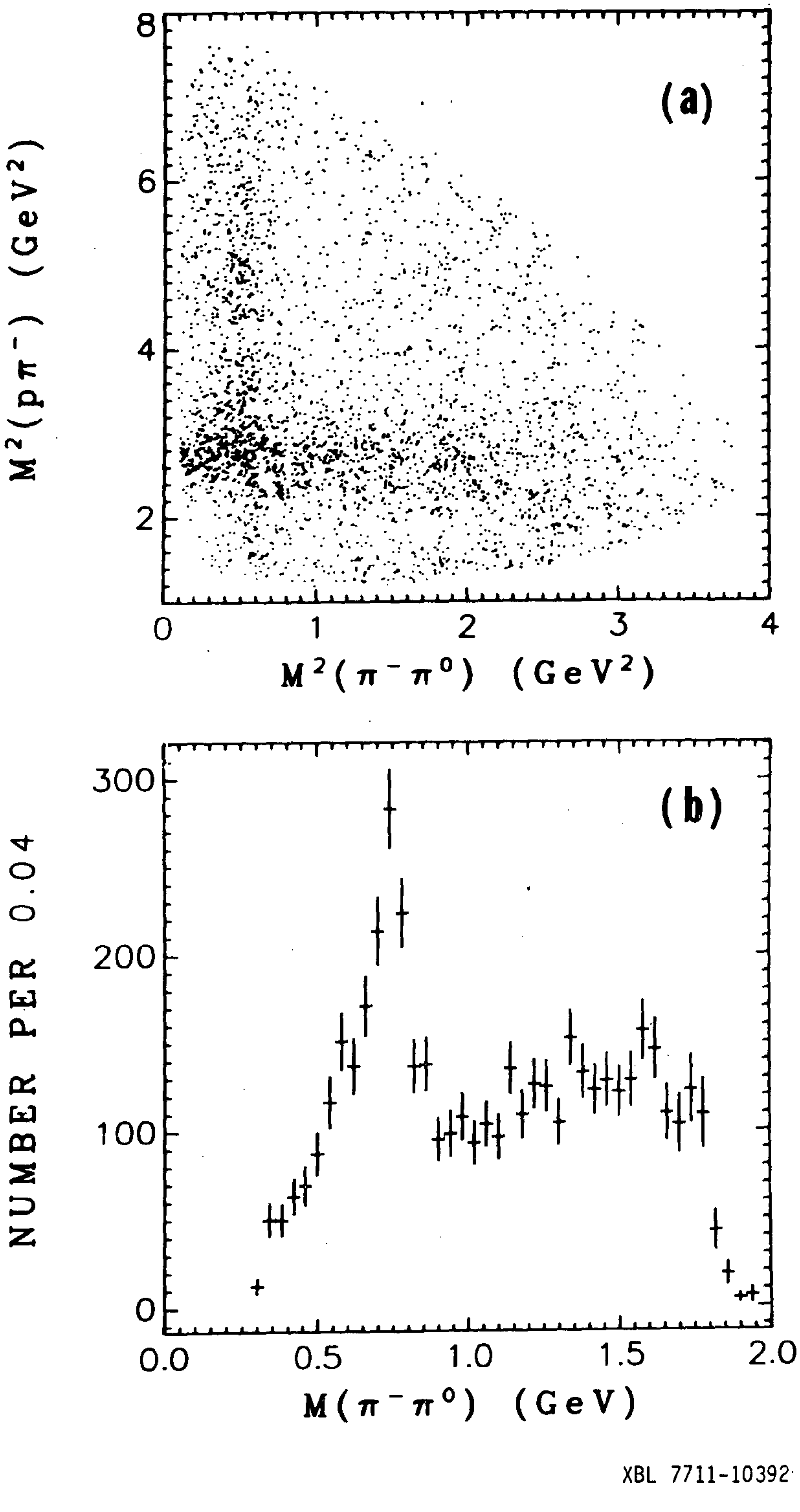
(a)
8
6
4
2
0
1
2
3
4
$M^2(p\pi^-)$ (GeV^2)
$M^2(\pi^-\pi^0)$ (GeV^2)
(b)
300
200
100
0
0.0
0.5
1.0
1.5
2.0
NUMBER PER 0.04
$M(\pi^-\pi^0)$ (GeV)
XBL 7711-10392

Fig. 1

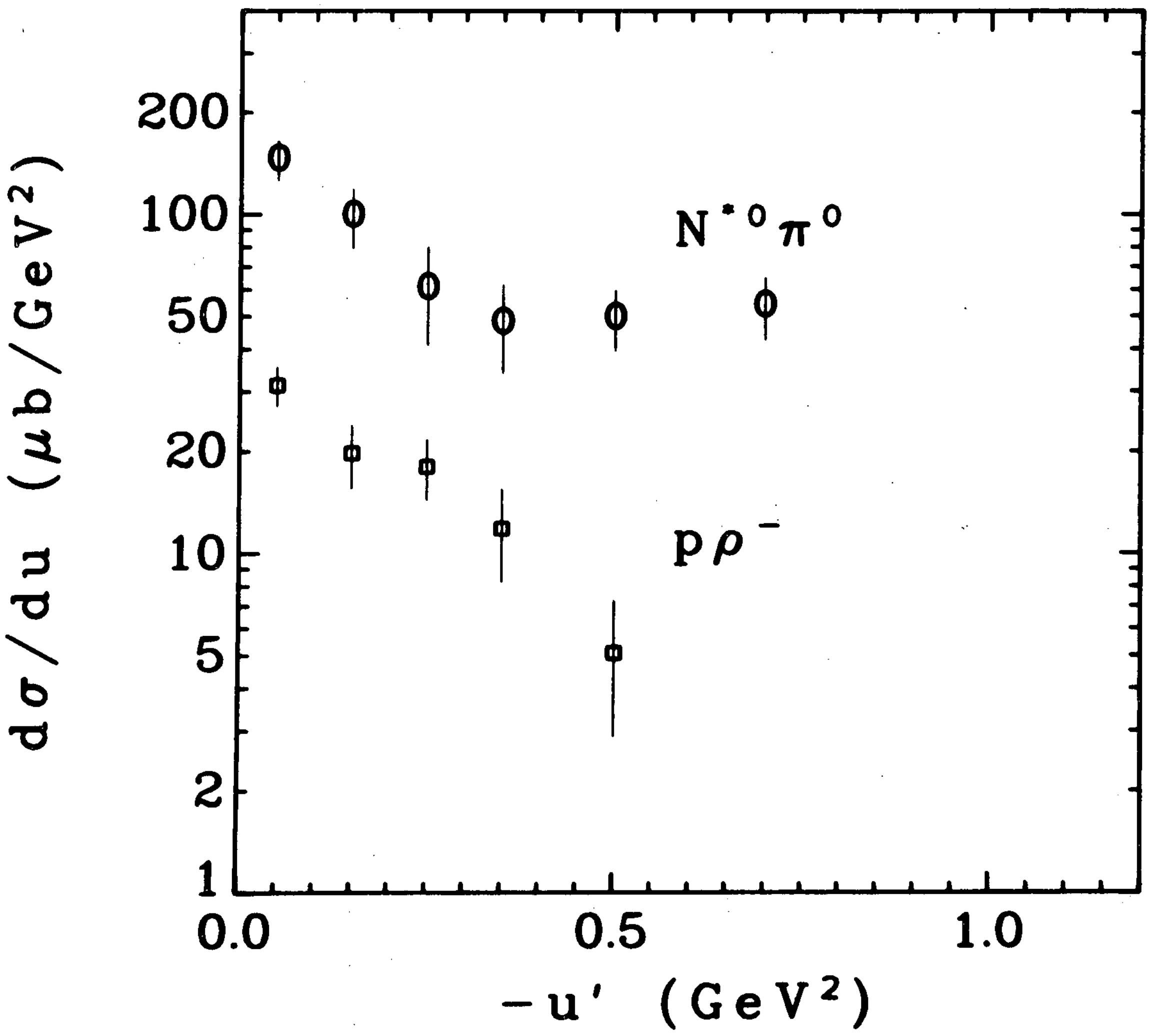

XBL 7712-10941

Fig. 2

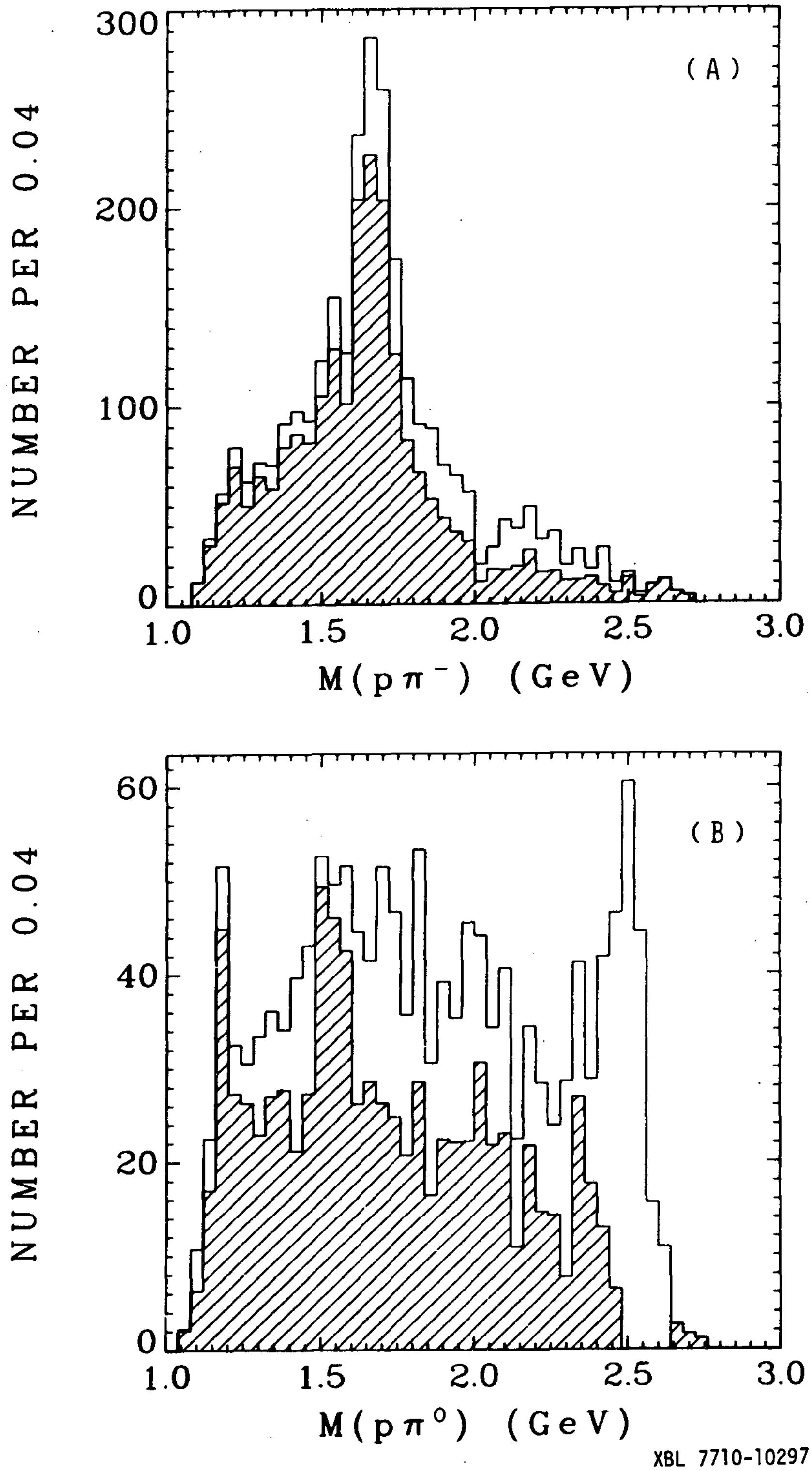
300
200
100
0
NUMBER PER 0.04
(A)
1.0
1.5
2.0
2.5
3.0
M(pπ⁻) (GeV)
60
40
20
0
NUMBER PER 0.04
(B)
1.0
1.5
2.0
2.5
3.0
M(pπ⁰) (GeV)
XBL 7710-10297

Fig. 3

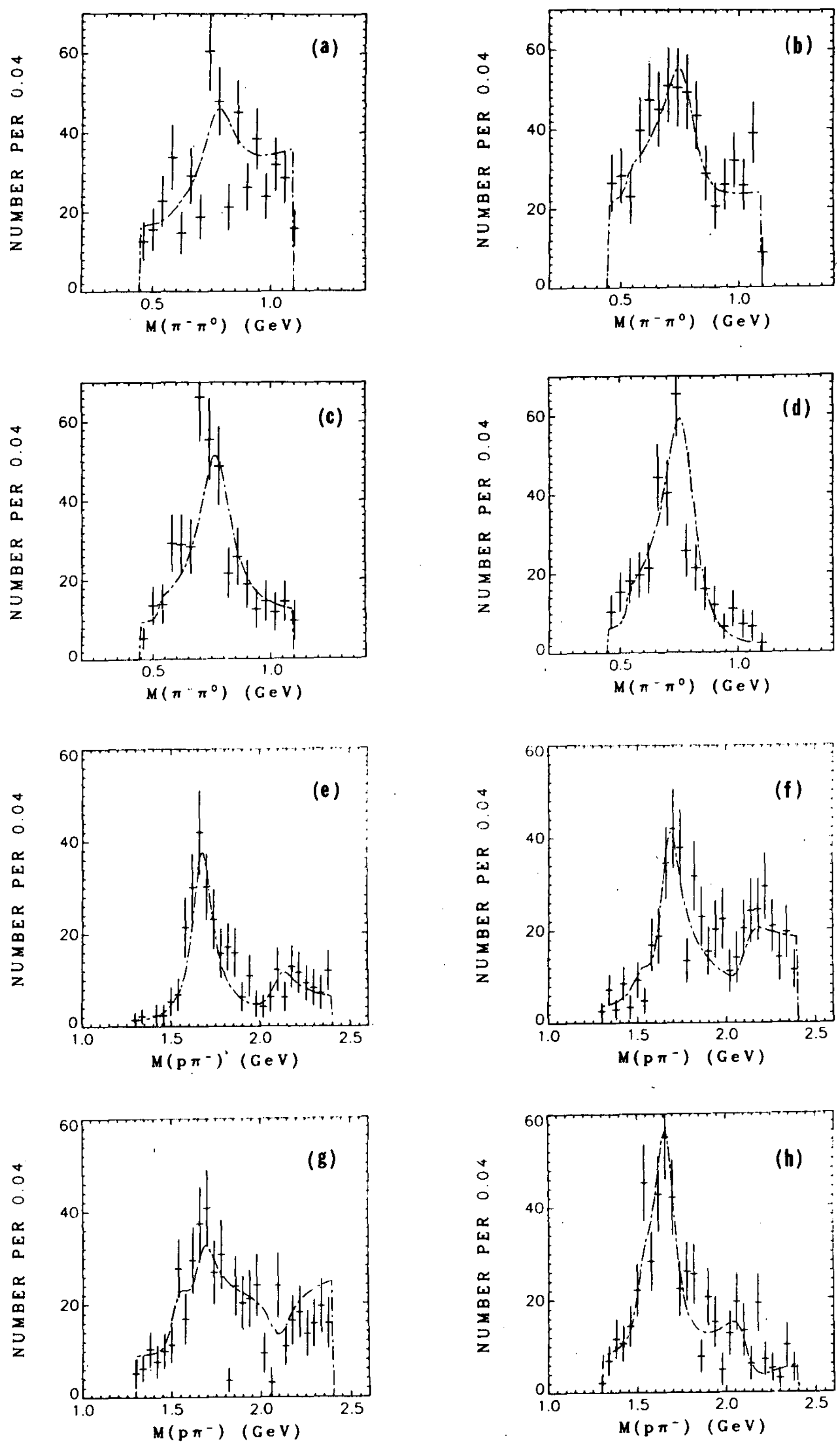

XBL 7711-10389

Fig. 4

0 0 0 0 4 8 0 7 4 2 3

TECHNICAL INFORMATION DEPARTMENT
LAWRENCE BERKELEY LABORATORY
UNIVERSITY OF CALIFORNIA
BERKELEY, CALIFORNIA 94720